This paper was recommended for publication in revised form by Regional Editor Mohamed Awad

NUMERICAL 3-D HEAT FLOW SIMULATIONS ON DOUBLE-PASS SOLAR COLLECTOR WITH AND WITHOUT POROUS MEDIA

*Abdel Illah Nabil KORTI
ETAP laboratory, University of Tlemcen, FT, Department of Mechanics,
BP 230, 13000 Tlemcen, Algeria

ABSTRACT

A transient 3-D mathematical model for double-pass solar collector with porous media in the lower channel has been developed. Numerical simulations model based on setting mass, momentum and energy balances on finite volumes method are carried out. The governing equations inside the two channels, together with the energy equation in the absorber, insulating and glass cover walls were solved iteratively in a segregated manner. Effects of porosity (70-90 %), mass flow (0.03-0.07 kg/s), solar intensity (514-714 W/m^2) and spacing glass-absorber-insulation (7-10 cm) on the dynamic and thermal behaviors of the double-pass solar collector with and without porous media have been discussed. The study concluded that the presence of the porous media at the bottom of the absorber is the best configuration and allow increasing the outlet temperature.

INTRODUCTION

A solar collector is an apparatus able to collect the solar irradiation and transmit heat to a working fluid which will transport it towards zones need to be heated. This mode of exploitation constitutes one of the most widespread techniques of this immense energy source. The advantages of this energy are: its renewable character, the absence of pollution and its exemption from payment (except expenses of installation and maintenance). On the other hand, the solar energy is intermittent (absent during the night), its intensity decreases with the presence of the clouds and the various areas of the earth do not receive same solar intensity according to their latitude or the season. Various designs of solar collectors have been the subject of many theoretical and experimental investigations for performance improvement. The most studies suggesting that the key parameter to improve the performance

is the heat transfer rate between the absorber plate and the flowing air. To meet this objective, many modifications have been proposed, including the use of finned, corrugated absorbers, oscillating flow, heat loss reduction and multiple-pass air flow configurations. Thus, double pass counter flow solar air collector with porous material in lower channel is one of the important design improvements used to improve the thermal performance.

Sopian et al [1] presented the thermal performance of a double-pass solar collector with and without porous media in the lower channel of the collector. The experimental study was undertaken under various designs and operating conditions. The study concluded that the changes in upper and lower channel depth, the mass flow rate, and solar irradiation intensity affect considerably the thermal efficiency of the double-pass solar collector. The study shows that the use of porous media increases the thermal efficiency of the systems. After, Sopian et al [2] develops a theoretical model for a double-pass solar collector. The porous media has been arranged in different porosities to increase heat transfer, area density, and the total heat transfer rate. This second study concluded that the proposed collector has a higher thermal performance compared to the conventional single-pass solar collector. Typical thermal efficiency of the double pass solar collector with porous media is about 60–70%. Moreover, the efficiency of the double-pass solar collector with porous media is 20-70% higher than the collector without porous media.

The heat transfer characteristics and performance of the double-pass flat plate solar air heater with and without porous media are studied numerically by Naphon [3]. The mathematical models described the heat transfer are derived from the energy conservation equations. The implicit method of finite-difference scheme is employed to solve these models.

The study shows that the porous media gives 25.9 % higher thermal efficiency than that without porous media.

Ho et al [4] presented the mathematical statement for a double-pass sheet-and-tube solar water heater and studies the external recycle effect on the collector efficiency. The study shows that the recycle effect can effectively enhance the collector efficiency compared to the single-pass device. It was found that the increment of convective transfer rate by increasing the recycle ratio could generally compensate for the decrement of the temperature difference, leading to improved performance. Also, the collector efficiency increases with increasing the tube length or decreasing the number of tube pairs for a specified collector area and the distance between tubes. After, the same authors [5] shows that the improvement in collector performance is obtained by employing a recycler operation with fins attached under various arrayed density, instead of employing a single-pass flat-plate device. The effect of the recycle ratio, arrayed density, and number of fins attached on the collector efficiency enhancement as well as the power consumption increment has also delineated. The study shows that the collector efficiency improvement increases with increasing distance between tubes, incident solar radiation, number of fins attached and inlet water temperature but with decreasing mass flow rate for smaller number of pair ducts.

Sebaa et al [6-7] investigated experimentally and theoretically the thermal performance of a double glass, double pass solar air heater with a packed bed. The simulations were performed by using limestone and gravel as packed bed materials. The study indicates that is preferable to use a packed bed of low porosity above the absorber plate. The best performance was obtained with gravel as a packing material when mass flow rate is 0.05 kg/s. The thermal efficiency with gravel was found to be 22–27% higher than that without the packed bed. The annual averages of the outlet temperature of air and thermal efficiency were found to be 16.5 % and 28.5 % higher than those for the system without the packed bed.

Ramani et al [8] presented theoretical and experimental analysis of double pass solar air collector with and without porous material. The results reveals that the thermal efficiency of double pass solar air collector with porous absorbing material is 20–25% and 30–35% higher than that of double pass solar air collector without porous absorbing material and single pass collector, respectively.

In the Ho et al [9] study, the double-pass device was constructed by inserting the absorbing plate into the air conduit to divide it into two channels. The collector was designed with heat transfer area double using the fins between the absorbing plate and heated air. Moreover, the advantage of external recycle application to solar air heaters is the enhancement of forced heat convection strength, resulting in considerable device heat transfer performance improvement. This advantage may compensate for the remixing at the inlet which decreases the heat transfer transfer-driving force decrement (temperature difference). The study concluded that more than 80% improvement in collector efficiency is obtained using the recycling operation.

Kumar et al [10] investigated a photovoltaic/thermal (PV/T) solar air heater with a double pass configuration and vertical fins in the lower channel. The fins are arranged perpendicularly to the direction of air flow to enhance the heat transfer rate and efficiency. The extended fin area reduces the cell temperature considerably, from 82 to 66 °C. The determined influenced of packing factor on the thermal, electrical and total equivalent thermal efficiencies indicate that a higher packing factor is useful for producing more electrical output per unit collector area and also in controlling the cell temperature, but marginally reduces thermal output.

Chamoli et al [11] presented an extensive study of the research carried out on double pass solar air heater. A number of analytical and experimental studies have been carried out with porous media (packed bed) and fins integrated double pass solar air heater which shows significant increase of the performance compared to the conventional system. Few studies were carried out with corrugated absorber. Further no study has been reported so far on double pass solar air heater with absorber plate artificially roughened from both the sides.

Hu et al [12] developed a numerical model to predict the internal flow and heat transfer characteristics in a solar air collector with internal baffles. The influence of baffle number, the thickness of air gap, the number of top glass cover and the operating conditions on the collector performance is was analyzed. The investigation results indicate that the introduction of baffles can strengthen the convective heat transfer process and lessen the radiation heat loss, which contributes to efficiency improvement. But the presence of baffles causes strong flow separation which results in flow loss to some extent.

Hernández et al [13] developed two analytical models that describe the thermal behavior of solar air heaters of double-parallel flow and double-pass in counter flow. The second model indicates that increasing the airflow increases the temperature rise in the inlet channel and the outlet air temperature may be lower than that existing in the central portion of the bottom channel of the collector. Therefore, for greater air mass flow, it is more convenient to use collectors of double-parallel flow than a double-pass counter flow one.

This paper presents numerical analysis of double pass solar air collector with porous material and compares his thermal performance with a classical double pass collector. A numerical model has been developed of enhanced forced convection in channels of collector. Darcy–Brinkman–Forchheimer flow model is used to characterize the thermo-flow fields inside the porous media. The majority of existing work in the literature of the double pass solar air collector with porous material [2, 11, 14] uses a mathematical models based on energy balance equations. This model assumes that the temperature of flowing air was varied only in the flow direction. In the present study the computational fluid dynamics (CFD) tool has been used to simulate a 3D transient model of the solar collector for better understanding dynamic and heat transfer capability.

SYSTEM DESCRIPTION AND MATHEMATICAL ANALYSIS

System description

The schematic of the double pass solar collector studied is shown in Fig. 1. The collector consists of the glass cover, the insulated container and the black painted aluminum absorber. The size of the collector is 120 cm wide and 240 cm long. In this type of collector, air enters at ambient temperature and warms up as it moves along the channel. The air circulates between the transparent cover and the absorber plate (upper channel) and turns back flowing between the absorber plate and the insulation base (lower channel). The porous media is envisaged below the absorber plate. Main thermal parameters of the materials used in the solar collector simulation are shown in Table 1.
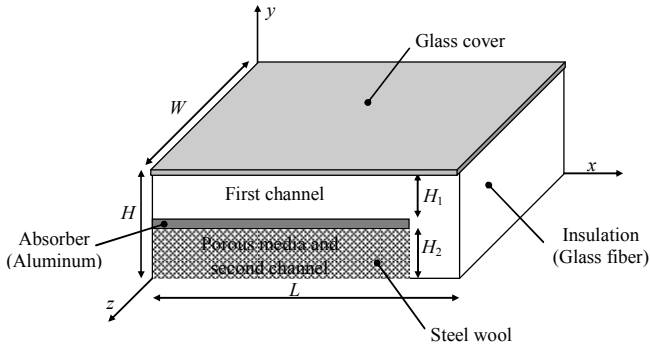
FIG. 1. SCHEMATIC OF THE DOUBLE PASS SOLAR COLLECTOR DESIGN.

Theoretical modeling

Mathematical formulation is based on three-dimensional, unsteady, laminar and incompressible flow with constant properties and negligible buoyancy effects. The governing equations for the fluid region are governed by the Navier–Stokes equations. The flow in the porous media is governed by Brinkman–ForchHeimer Extended Darcy model.

The governing equations for the fluid region can be written as:

Continuity equations

$$\frac{\partial u}{\partial x} + \frac{\partial v}{\partial y} + \frac{\partial w}{\partial z} = 0 \tag{1}$$

Momentum equations in x, y and z directions, respectively, have the following forms:

$$\rho_f \left(\frac{\partial u}{\partial t} + u\frac{\partial u}{\partial x} + v\frac{\partial u}{\partial y} + w\frac{\partial u}{\partial z} \right) = \\ -\frac{\partial P}{\partial x} + \mu_f \left(\frac{\partial^2 u}{\partial x^2} + \frac{\partial^2 u}{\partial y^2} + \frac{\partial^2 u}{\partial z^2} \right) \tag{2}$$

$$\rho_f \left(\frac{\partial v}{\partial t} + u\frac{\partial v}{\partial x} + v\frac{\partial v}{\partial y} + w\frac{\partial v}{\partial z} \right) = \\ -\frac{\partial P}{\partial y} + \mu_f \left(\frac{\partial^2 v}{\partial x^2} + \frac{\partial^2 v}{\partial y^2} + \frac{\partial^2 v}{\partial z^2} \right) \tag{3}$$

$$\rho_f \left(\frac{\partial w}{\partial t} + u\frac{\partial w}{\partial x} + v\frac{\partial w}{\partial y} + w\frac{\partial w}{\partial z} \right) = \\ -\frac{\partial P}{\partial z} + \mu_f \left(\frac{\partial^2 w}{\partial x^2} + \frac{\partial^2 w}{\partial y^2} + \frac{\partial^2 w}{\partial z^2} \right) \tag{4}$$

Energy equation

$$(\rho c)_f \left(\frac{\partial T_f}{\partial t} + u\frac{\partial T_f}{\partial x} + v\frac{\partial T_f}{\partial y} + w\frac{\partial T_f}{\partial z} \right) = \\ \lambda_f \left(\frac{\partial^2 T_f}{\partial x^2} + \frac{\partial^2 T_f}{\partial y^2} + \frac{\partial^2 T_f}{\partial z^2} \right) \tag{5}$$

For flow and heat transfer in the convective porous media, the governing equations can be written as:

Continuity equation

$$\frac{\partial u}{\partial x} + \frac{\partial v}{\partial y} + \frac{\partial w}{\partial z} = 0 \tag{6}$$

Momentum equations in x, y and z directions, respectively, have the following forms [15-17]:

$$\frac{\rho_f}{\varepsilon} \left(\frac{\partial u}{\partial t} + u\frac{\partial u}{\partial x} + v\frac{\partial u}{\partial y} + w\frac{\partial u}{\partial z} \right) = -\frac{\partial P}{\partial x} \\ + \mu_{eff} \left(\frac{\partial^2 u}{\partial x^2} + \frac{\partial^2 u}{\partial y^2} + \frac{\partial^2 u}{\partial z^2} \right) - \left(\frac{\mu_f}{k} + \frac{\rho_f F \varepsilon}{\sqrt{k}} u \right) u \tag{7}$$

$$\frac{\rho_f}{\varepsilon} \left(\frac{\partial v}{\partial t} + u\frac{\partial v}{\partial x} + v\frac{\partial v}{\partial y} + w\frac{\partial v}{\partial z} \right) = -\frac{\partial P}{\partial y} \\ + \mu_{eff} \left(\frac{\partial^2 v}{\partial x^2} + \frac{\partial^2 v}{\partial y^2} + \frac{\partial^2 v}{\partial z^2} \right) - \left(\frac{\mu_f}{k} + \frac{\rho_f F \varepsilon}{\sqrt{k}} v \right) v \tag{8}$$

$$\frac{\rho_f}{\varepsilon} \left(\frac{\partial w}{\partial t} + u\frac{\partial w}{\partial x} + v\frac{\partial w}{\partial y} + w\frac{\partial w}{\partial z} \right) = -\frac{\partial P}{\partial z} \\ + \mu_{eff} \left(\frac{\partial^2 w}{\partial x^2} + \frac{\partial^2 w}{\partial y^2} + \frac{\partial^2 w}{\partial z^2} \right) - \left(\frac{\mu_f}{k} + \frac{\rho_f F \varepsilon}{\sqrt{k}} w \right) w \tag{9}$$

TABLE 1. MATERIAL PARAMETERS USED IN THE SOLAR COLLECTOR MODELS

	Density (Kg/m^3)	Specific heat (J/(kgK))	Thermal conductivity (W/(mK))	Absorptivity	Transmitivity	Emissivity	Thickness (mm)
Glass cover	1375	840	0.96	0.06	0.92	0.92	4
Aluminum	2719	871	202.4	0.95			2.5
Glass fiber	15	800	0.04				50
Steel wool	15	452	25				

where p is the pressure, μ_{eff} is the effective dynamic viscosity of the fluid, μ_f is the dynamic viscosity of the fluid, k is the permeability and F is the inertia coefficient of the porous media described by Kozeny-Carman correction equation. For the porous layer of particle diameters d_p and porosity ε [16-17]:

$$\mu_{eff} = \frac{\mu_f}{\varepsilon} \qquad (10)$$

$$k = \frac{d_p^2 \, \varepsilon^3}{150\left(1-\varepsilon^2\right)} \qquad (11)$$

$$F = \frac{1.75}{\sqrt{150} \, \varepsilon^{3/2}} \qquad (12)$$

Fluid-phase energy equation:

$$(\rho c)_{eff}\left(\frac{\partial T_f}{\partial t} + u\frac{\partial T_f}{\partial x} + v\frac{\partial T_f}{\partial y} + w\frac{\partial T_f}{\partial z}\right) = \\ \lambda_{eff}\left(\frac{\partial^2 T_f}{\partial x^2} + \frac{\partial^2 T_f}{\partial y^2} + \frac{\partial^2 T_f}{\partial z^2}\right) \qquad (13)$$

Solid-phase energy equation:

$$(\rho c)_{eff}\left(\frac{\partial T_s}{\partial t}\right) = \lambda_{eff}\left(\frac{\partial^2 T_s}{\partial x^2} + \frac{\partial^2 T_s}{\partial y^2} + \frac{\partial^2 T_s}{\partial z^2}\right) \qquad (14)$$

In above equations, T_f and T_s are, respectively, the fluid and solid matrix temperatures. The effective density and specific heat $(\rho c)_{eff}$ is calculated as following:

$$(\rho c)_{eff} = \varepsilon(\rho c)_f + (1-\varepsilon)(\rho c)_f \qquad (15)$$

and the effective thermal conductivity is calculated as following:

$$\lambda_{eff} = \varepsilon\lambda_f + (1-\varepsilon)\lambda_f \qquad (16)$$

Boundary conditions and initial conditions

The Numerical simulations are solved for a typical hot day for Tlemcen (Algeria) climatic conditions during July. Hourly outdoor ambient temperature variation used in solving the model is given in (Fig. 2.a) by [18]:

$$T_a(t) = \overline{T_a} + T_r \cos\left[\frac{\pi}{12}(t-14)\right] \qquad (17)$$

where $\overline{T_a}$ is the average outdoor ambient temperature of 28°C and T_r is the amplitude of 6°C. The measured hourly average solar intensity $G(t)$ and used in solving the model is given in (Fig. 2.b).

Initially, the fluid inside the solar collector is supposed at rest (velocities are fixed at zero) with a temperature equal to the ambient temperature. The associated boundary conditions for the solar collector are given as:

Inlet boundary condition: The uniform velocity is given at the inlet of the solar collector.
At $x = 0$, $H_2 + \delta_{ab} \le y \le H_2 + \delta_{ab} + H_1$, $0 \le z \le W$

$$u = u_{in}, \; v = w = 0, \; T_f(t) = T_a(t) \qquad (18)$$

Outlet boundary condition: The fully developed conditions are satisfied.
At $x = 0$, $0 \le y \le H_2$, $0 \le z \le W$

$$\frac{\partial u}{\partial x} = \frac{\partial v}{\partial x} = \frac{\partial w}{\partial x} = \frac{\partial T}{\partial x} = 0 \qquad (19)$$

Wall boundary conditions: No slip conditions employed at inner side of the solar collector wall surface. At the exterior of the solar collector, the surfaces are exposed to the combined external convection and radiation boundary conditions.
At the glass surface:

$$\lambda\left(\frac{\partial T}{\partial n}\right)_{wall} = h(T_a - T_w) + \varepsilon_g\sigma\left(T_{sky}^4 - T_w^4\right) + G \qquad (20)$$

At the others surfaces:
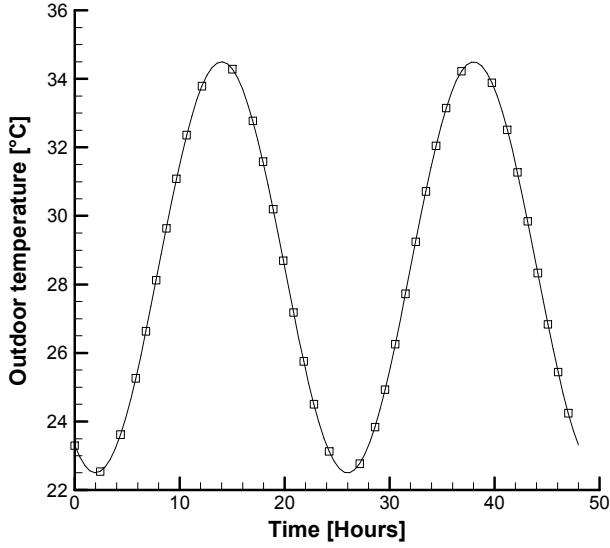
(a)
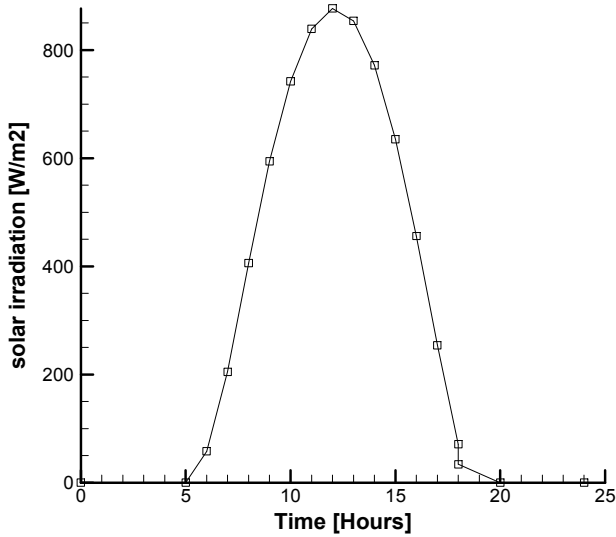
(b)

FIG. 2. HOURLY AVERAGE (a) OUTDOOR AMBIENT TEMPERATURE AND (b) SOLAR INTENSITY.

$$\lambda \left(\frac{\partial T}{\partial n} \right)_{wall} = h \left(T_a - T_w \right) + \varepsilon_{ext} \sigma \left(T_{sky}^4 - T_w^4 \right) \tag{21}$$

The convective heat transfer coefficient for air wind and the sky temperature can be found in [19] as:

$$h = 2.8 + 3.0V \tag{22}$$

$$T_{sky} = 0.0552 \left(T_a \right)^{1.5} \tag{23}$$

where V is the average wind velocity and taken 1.27 m/s.

The thermal efficiency of solar air heater can be expressed as:

$$\eta = \frac{q_m c_f \left(T_o - T_i \right)}{GA} \tag{24}$$

NUMERICAL SOLUTION

To solve the governing equations numerically, the FLUENT software based on the finite volume method (FVM), is employed with additional subroutines incorporated (UDF's) for specifying unsteady state boundary conditions. The discretization of the equations is fully conservative and time implicit. The PISO (Pressure Implicit with Splitting of Operators) algorithm is used to couple the pressure and velocity. This algorithm is simply recognized as an extension of SIMPLE with an additional corrector step that involves an additional pressure correction equation to enhance the convergence. The PISO algorithm takes relatively more CPU time per solver iteration, but it significantly decrease the number of iterations required for the convergence of the transient flow problems. Non-uniform mesh sizes were used for the numerical computation. To test the grid independence, several different grid sizes had been tested in the present study (Fig. 3). The numbers of grid retained were 239,400 cells with 265,225 nodes. As far as the unsteady-state numerical calculations, the time step was concerned and several values of Δt had been examined for the grid size chosen. Hence, the time step of $\Delta t = 45$ s were used for the unsteady-state numerical calculations performed in this study. A HP Z210 Workstation Intel Xeon (3.2 GHz) was used for all the simulations, requiring about 7 minutes of Central Processing Unit (CPU) time. The convergence is checked at each time-step and convergence criteria are the scaled residuals less than 10^{-4} for all equations.
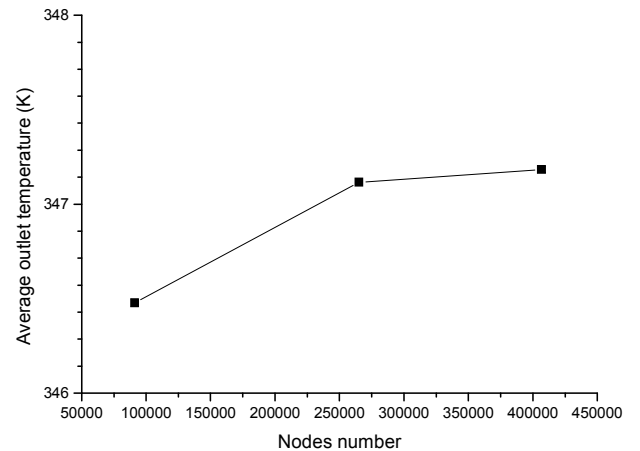
FIG. 3. TEST OF THE GRID INDEPENDENCE.
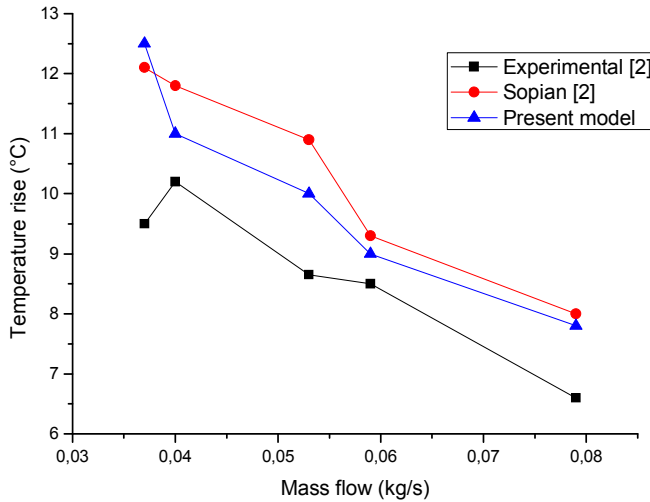
FIG. 4. COMPARISON BETWEEN THE EXPERIMENTAL, NUMERICAL AND PRESENT MODEL.

To verify the precision of the developed numerical model we propose to compare the obtained results with those obtained in the literature who studied a double pass solar collector with porous media. Fig. 4 shows a comparison between the evolutions of the air temperature rise at various masse flow obtained numerically with the new model proposed and those predicted experimentally and numerically by Sopian [2]. A comparison shows that there is excellent correlation with that obtained by the present method. This underlines the good accuracy of the method proposed in this work.

PARAMETRIC STUDY OF THE SOLAR COLLECTOR

To see the effect of the parameters (solar intensity, mass flow and spacing glass-absorber-insulation) it is preferable to consider the problem in steady state. For this, we consider the problem as steady state in this first part.

The flow pattern in the collector influences the temperature distribution significantly. The temperature contours and the velocity vectors of the middle cross-section ($z = 0.6$ m) are shown in Fig. 5. As expected, the air temperature increases along the length of the solar air collector. The Fig. 5.a shows that the hottest areas of the air in the collector correspond to the presence of the recirculation zones. The recirculation zones cause a local rotation of the air which promotes the heat transfer by conduction and reduces the heat dissipation by heat convection flow. However, the least hot areas correspond to the direct laminar flow. Without porous media, we notice that the temperature difference between the absorber and the air is more important. With the presence of the porous media, the results show that this temperature difference decreases. Indeed, the porous media increases the heat flow exchanged between the absorber plate and the air flow. Consequently, the absorber temperature decreases and the air flow temperature increases.

Without porous media, the air temperature in the first channel is more important than that of the collector with porous media. However, the air temperature in the second channel is more important for the collector with porous media. The porous media allows increasing the heat flux transferred from the absorber towards the air in the second channel. This increasing involves the reduction in the heat flux transferred from the absorber towards the air in the first channel. Thus, the porous media allows improving the transfer of irradiation heat absorbed by the absorber towards the air in the second channel. We can say that the absorbed solar irradiation is distributed between the absorber and the porous media. Consequently, the absorber temperature decreases and the air temperature in the second channel increases. This phenomenon causes the increase of the outlet air temperature, and thus, the collector thermal efficiency can increases.

Fig. 6 shows the variations of the equivalent heat transfer coefficient (W/(m²K)) at the lower surface of the absorber. As expected, the solar air heater with the porous media gives more than 10% higher heat transfer rate than that without porous media. This is because the heat transfer area of the solar air heater with porous media is higher than that without porous media. At the entrance of the second channel, the abrupt change in the flow direction involves a great fluctuation in the heat transfer coefficient. The increasing of the coefficient shows the dominance of the convection compared to the conduction and vice versa. At the outlet, the flow becomes more stable and the vortices disappear. Thus, the fluctuations disappear and the heat transfer coefficient decrease gradually.
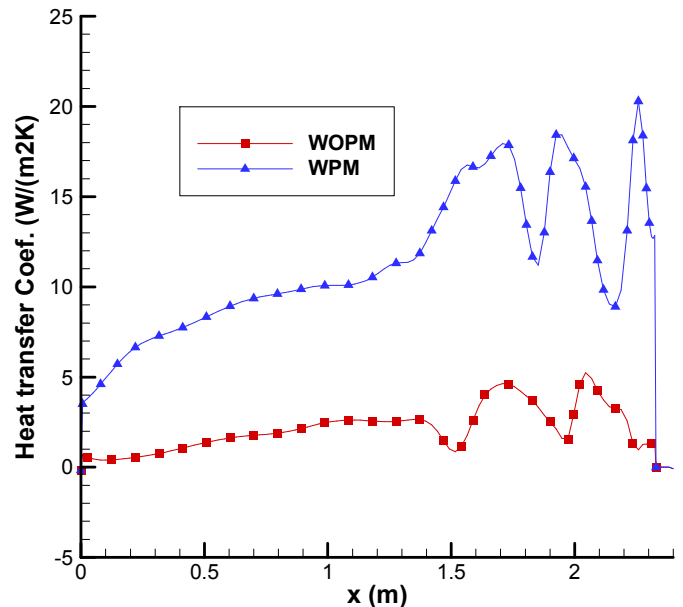
FIG. 6. VARIATIONS OF THE EQUIVALENT HEAT TRANSFER COEFFICIENT (W/(m²K)).
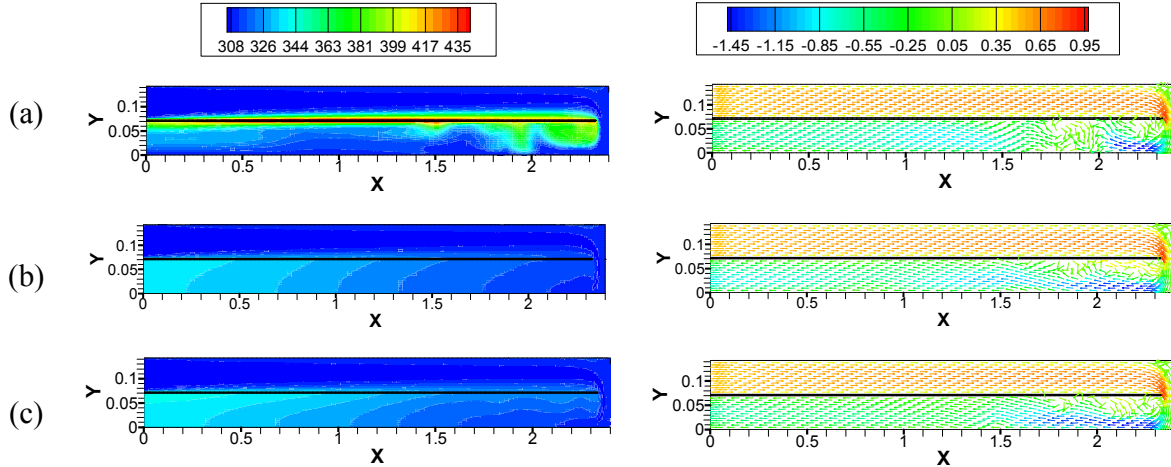
FIG. 5. ISOTHERMS AND VELOCITY VECTORS AT z **= 0.6 m FOR** G **= 614 W/m² (a) WITHOUT POROUS MEDIA (b) AND (c) WITH POROUS MEDIA FOR** ε **= 0.7 AND 0.9. BOTH AXES (m).**

To see the ratio of the predominance of the convection compared to the conduction, it is useful to trace the evolution of the Nusselt number at the lower surface of the absorber plate (Fig. 7). At the entrance of the second channel the Nusselt number increases quickly showing the predominance of the convection. The Nusselt number decreases after showing the presence of a first recirculation zone where the heat flow becomes dominated by conduction. After two other fluctuations the Nusselt number gradually decreases until the exit. The conduction gradually dominates the heat transfer compared to the convection by effect of the reduction of velocity. However, the figure shows that the presence of the porous media reduces considerably the Nusselt number. Indeed, the porous matrix has as a role to increase the heat conduction. With porous media, the fluctuations are less important and the heat transfer is more homogeneous.
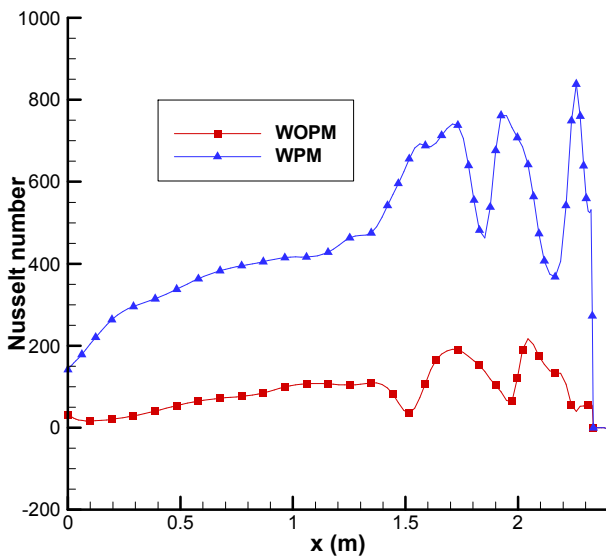
Fig. 8 shows temperature distributions in x direction at the center of the first and the second channel of solar collector. Clearly, we can see that the air temperature in the first channel is more important in the collector without porous media compared to the collector with porous media. In the second channel, we notice that the porous media offers a better increase in the air temperature and the air leaves the collector with a higher temperature. The temperature distributions with porous media in the second channel are more stable than that without one. The porous media contributes to improve the conduction heat transfer in the fluid flow and provides the reduction of fluctuations, and so, a more homogeneous temperature distributions. The figure shows that a porosity of 90% provides a better heat exchange between the absorber and the air compared to a porosity of 70%. Thus, the increase in porosity involves the increase of the air temperature in the second channel.

The outlet temperature investigation is an important parameter for applications. Fig. 9 shows the outlet temperature distributions in y direction at the center of the second channel of solar collector. Without porous media the air temperature in the vicinity of the absorber plate is significantly higher than that in the bottom and the temperature gradient is enough large. By using the porous media, the average outlet temperature is better and the temperature is almost constant. By increasing the porosity, the convection heat transfer is intensified and the conduction heat transfer is decreased. Since the heat convection is faster than the heat conduction, the increase in the media porosity involves the increase in the air temperature. The Figure shows that a porosity of 90% provides higher heat exchange than that 70%. The porous media of 90% porosity gives the higher outlet temperature of air.

FIG. 7. VARIATIONS OF THE NUSSELT NUMBER.
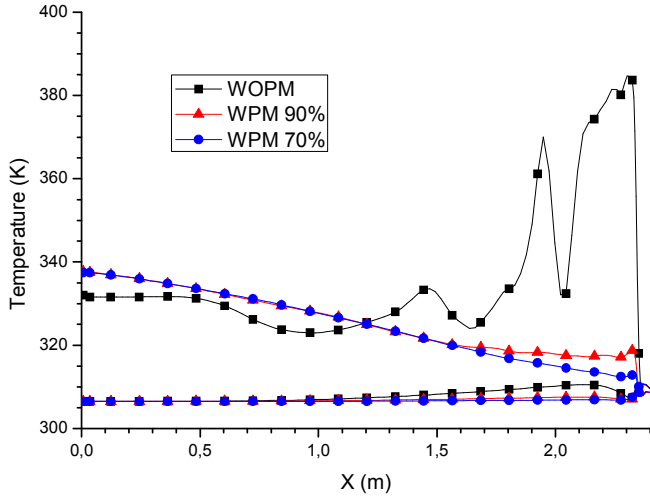
FIG. 8. THE AVERAGE TEMPERATURES DISTRIBUTIONS OF AIR IN *x* DIRECTION AT THE FIRST AND THE SECOND CHANNEL.
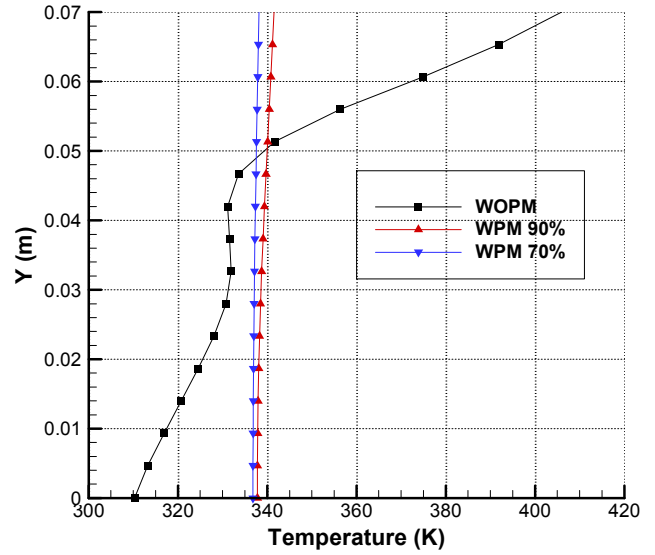
FIG. 9. THE OUTLET TEMPERATURE DISTRIBUTIONS OF AIR IN *y* DIRECTION AT THE SECOND CHANNEL.

(a)

(b)

(c)

Without porous media

With porous media
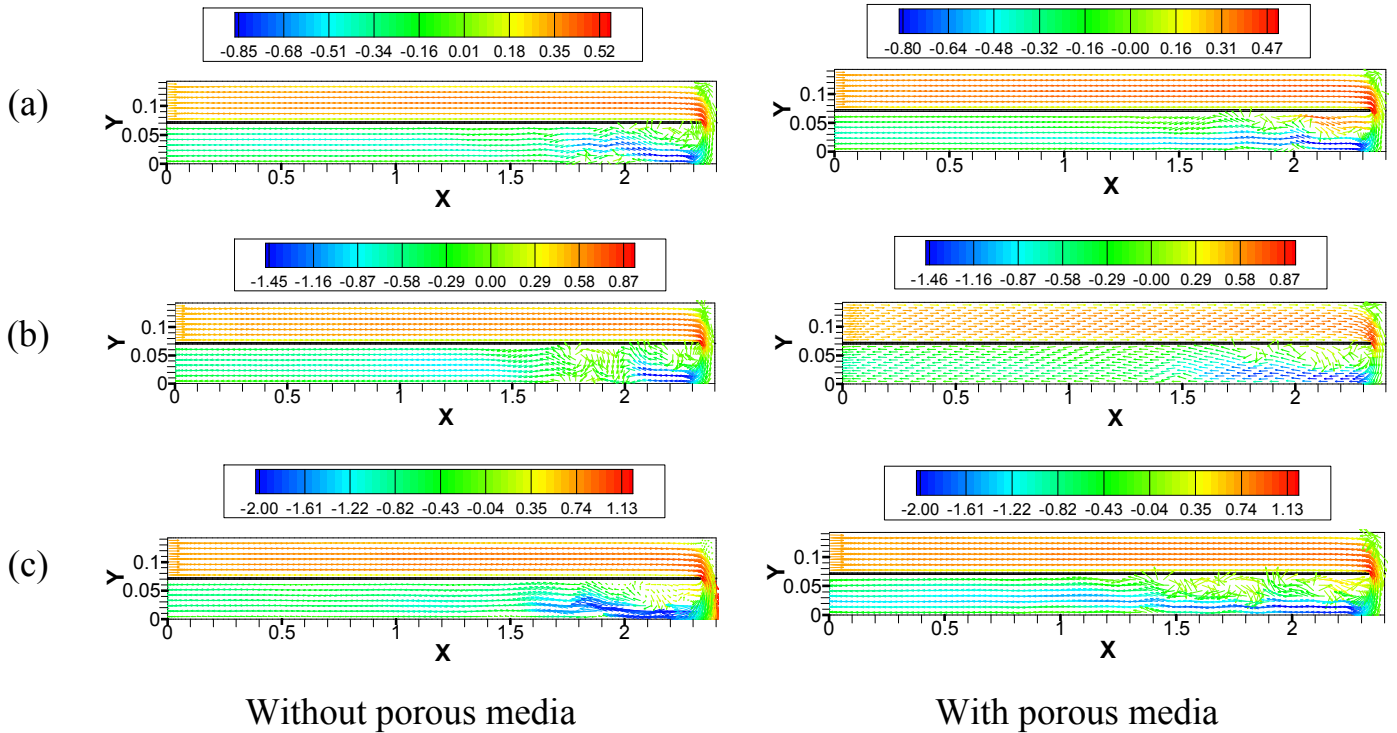
FIG. 10. MASS FLOW EFFECT ON THE CENTERLINE (*z* = 0.6 m) VELOCITY VECTORS EVOLUTION OF SOLAR COLLECTOR (a) 0.03 (b) 0.05 AND (c) 0.07 kg/s. BOTH AXES (m).
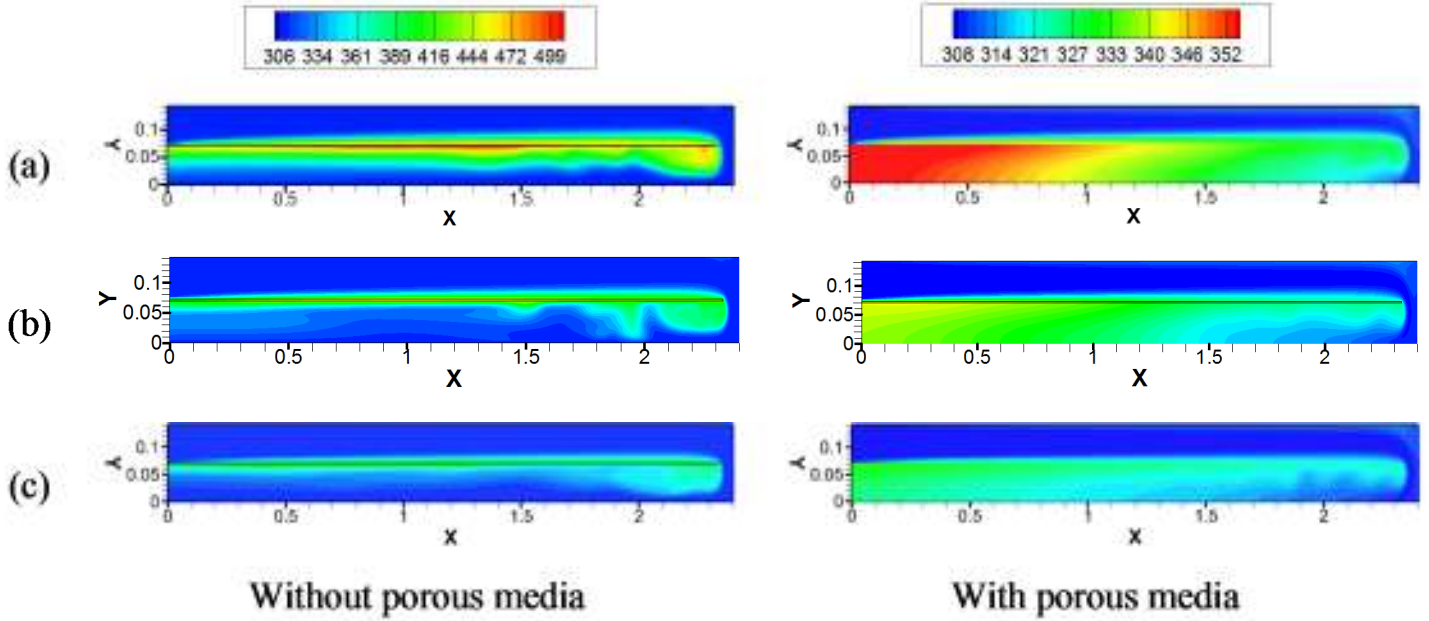
FIG. 11. MASS FLOW EFFECT ON THE CENTERLINE (z = 0.6 m) TEMPERATURE EVOLUTION OF SOLAR COLLECTOR (a) 0.03 (b) 0.05 AND (c) 0.07 kg/s. BOTH AXES (m).

Figs. 10 and 11 show the variations of velocity vectors and temperature contours with mass flow rate. With increased mass flow the velocity increases in the two channels of solar collector at a specific porosity (90%). Without porous media, the recirculation zone existing at the inlet of the second channel becomes wider and passes from 0.4 to 0.6 cm when the mass flow increases from 0.03 to 0.07 kg/s. With the porous media, this recirculation zone is significantly reduced, but the flow becomes significantly disturbed in this region by increasing mass flow rate. The figures show that the mass flow influences considerably the dynamic and thermal behaviors of the solar collector. The higher mass flow rate reduces the air temperature at the outlet of the air and the temperature difference between the inlet and the outlet of air decreases. Decreasing the mass flow increases the residence time of the fluid in the two channels which causes an increase in the time to heat exchange with the absorber.
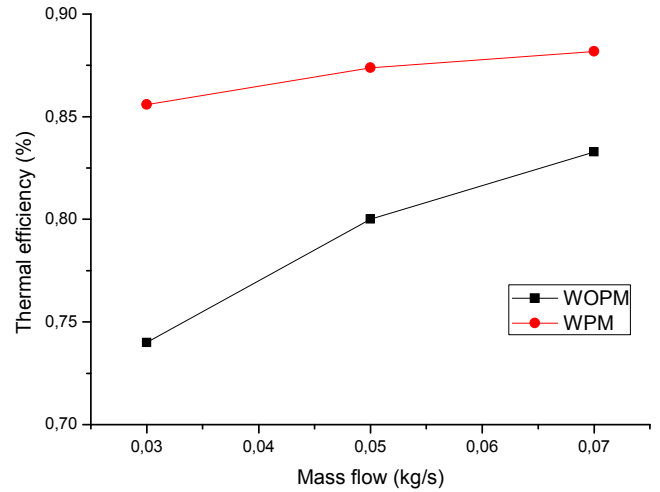
FIG. 12. MASS FLOW EFFECT ON THE THERMAL EFFICIENCY

18
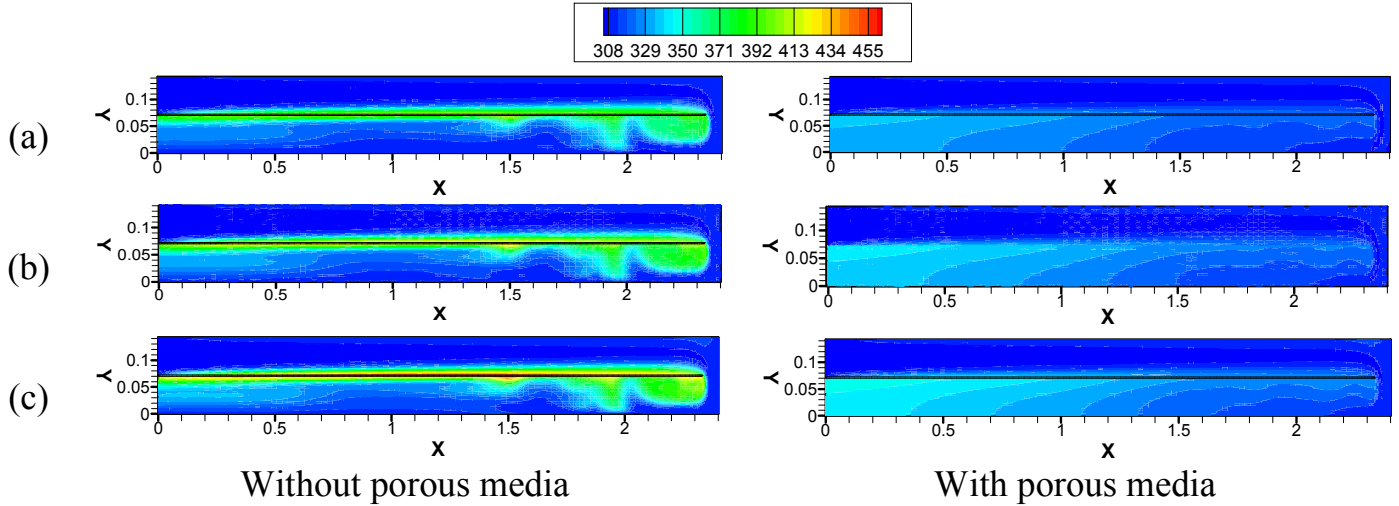
FIG. 13. SOLAR INTENSITY EFFECT ON THE CENTERLINE (z = 0.6 m) Temperature Evolution Of Solar Collector (a) 514 W/m² (b) 614 W/m² AND (c) 714 W/m². BOTH AXES (m).

Fig. 12 shows the mass flow effect on the collector thermal efficiency. We can see clearly that the porous media contributes to the improvement of the collector thermal efficiency. For a mass flow of 0.03 kg/s the porous media improves the thermal efficiency by about 13.5 %. This improvement of the thermal efficiency decreases with the increase of the mass flow and reaches about 5.5 % for a mass flow of 0.07 kg/s. The mass flow influences considerably the thermal efficiency of the collector without porous media. For the collector with porous media this influence is definitely less important.

Fig. 13 shows the solar intensity effect on the centerline (z = 0.6 m) temperature evolution of solar collector. The temperature rise is proportional to the solar irradiation intensity at a specific mass flow rate (0.05 kg/s). An increase in solar intensity increases the absorber temperature and consequently increases the air temperature. However, we can observe that with porous media the increase in the outlet air temperature is much better than without porous media. This shows that the use of the porous media can increases the thermal efficiency of the solar collector. For this, when the solar intensity becomes more intense the outlet air temperature becomes higher with the use of porous media.

Fig. 14 shows the solar intensity effect on the average absorber temperature. As mentioned previously, the average absorber temperature increases linearly with the increase in the solar intensity. We can see clearly that the presence of the porous media reduced considerably the absorber temperature. Indeed, the porous media absorbs the heat of the absorber plate and thus reduces its temperature. However, the increase of the

absorber temperature is less important with the presence of the porous media at a lower of the absorber plate. More solar irradiation is intense, more rate of the heat flow absorbed by the porous media is important. The thermal efficiency of the addition of the porous media is better for the weak solar irradiation.
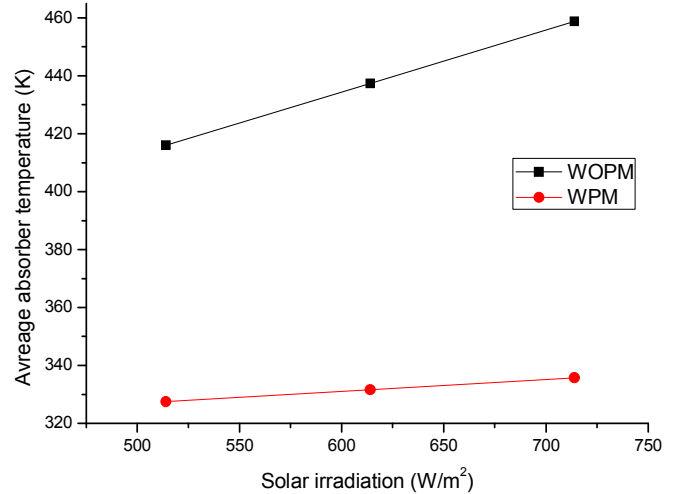
FIG. 14. SOLAR INTENSITY EFFECT ON THE AVERAGE ABSORBER TEMPERATURE.
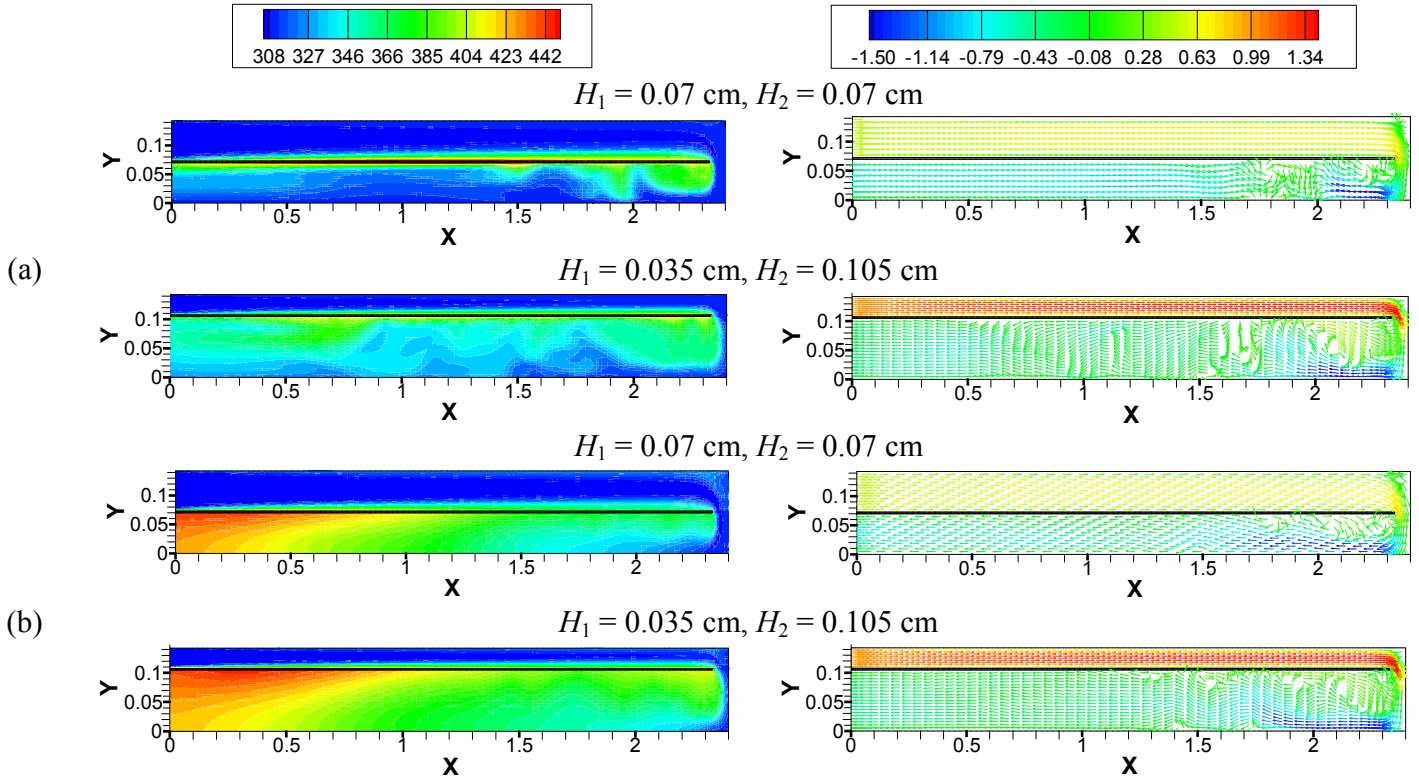
FIG. 15. SPACING GLASS-ABSORBER-INSULATION EFFECT ON THE CENTERLINE ($z = 0$) TEMPERATURE AND VELOCITY EVOLUTION OF SOLAR COLLECTOR (a) WITHOUT AND (b) WITH POROUS MEDIA. BOTH AXES (m).

Fig. 15 show the spacing glass-absorber-insulation effect on the centerline ($z = 0.6$ m) temperature contours and velocity vectors evolution of solar collector without and with porous media. For a constant mass flow rate, changing the channel height (and thus the channel section) involves a change of flow velocity. Fig. 10 showed that the velocity flow influences considerably the thermal behavior of the collector.

Decreasing glass-absorber spacing involves the increasing of the mean air velocity in the first channel and the air temperature decreases. However, increasing absorber-insulation spacing involves the reduction of the mean air velocity in the second channel and the air temperature increases. Since, we seek to decrease the thermal losses to the top and to increase heat exchange to the bottom; the reduction of upper spacing and the increasing of lower spacing seem very practical. With the increase of the spacing between the absorber and the insulating plate, the recirculation zone at the inlet of the second channel becomes wider and higher. The conduction heat transfer characterized by the recirculation phenomenon becomes more important and the heat flow transferred from the absorber to the air increase which leads to an increase in the temperature of the circulating air. However, we can see that, without porous media, the increasing of the outlet air temperature with increasing the spacing absorber-insulating plate is much higher than with porous media. This shows that the porous media increases sufficiently the conduction heat

transfer with a reduced spacing. Therefore, increase the spacing absorber-insulating plate in the case with porous media is not very practical

UNSTEADY OPERATION

Daily solar energy transmission through the solar collector will certainly create a significant temperature difference through the heater. For this, we propose to study the thermal behavior of the solar collector during the variation of the solar irradiation (unsteady state).

Fig. 16 shows the temperature contours variation of solar collector components as a result of daily solar intensity variation. The figure indicates the significant temperature changes corresponding to solar intensity variations. Further, as intensity increases, there is an increase in all temperatures. During all the day, we notice that the absorber records the most important temperature in the collector. Indeed, because of its radiation characteristic, the absorber can absorb the majority of the solar irradiation. The good thermal conductivity of the absorber allows a fast storage of the solar irradiation and a fast transfer of stored heat towards the air flow. Thus, the figure shows the great change of thermal behavior of the collector with the variation of the solar intensity during the day.
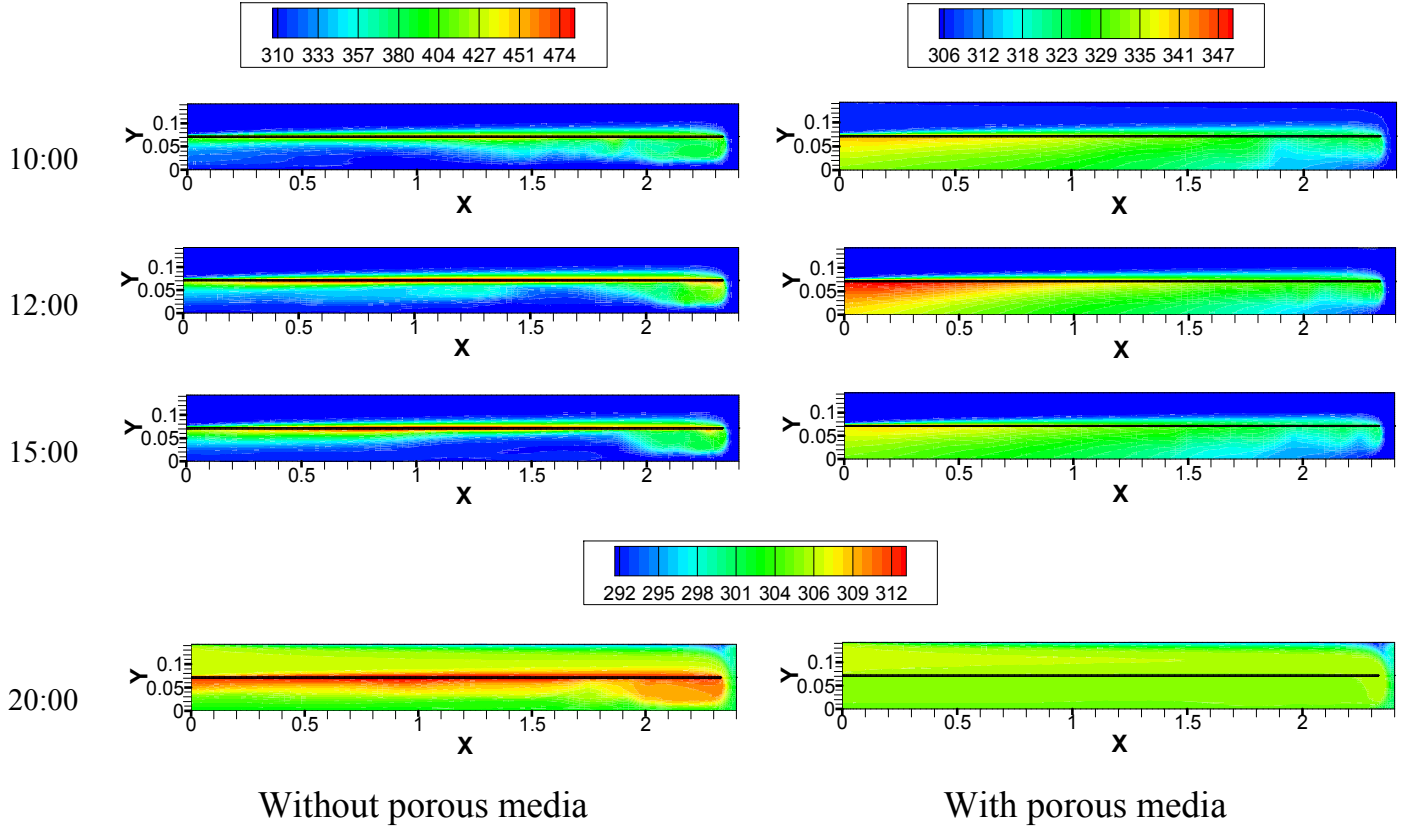
FIG. 16. EVOLUTION OF TEMPERATURE CONTOURS OF SOLAR COLLECTOR COMPONENTS AS A RESULT OF DAILY SOLAR INTENSITY VARIATION. BOTH AXES (m).

At sunshine and during the heating phase (05:00–12;00), the temperature of the different components of the solar collector increase continuously until reaching a maximum temperature in the midday at the absorber about 485°C and 347°C without and with porous media, respectively (Fig. 16).

Later in the day, at sunset and during the cooling phase (12:00–20:00), the solar radiation decreases and the temperature in the solar collector drop. It is noticed that the outlet air temperature is higher than the ambient temperature after sunset due to the storage effect of the absorber and the porous media. Comparison between the values of the outlet air temperature with and without the porous media, Fig. 17 indicates that the maximum values of the outlet air temperature with porous media are less than without porous media during sunshine hours. However, the outlet air temperature with porous media tends to decrease less rapidly during sunset. It may be concluded that to increase the outlet air temperature of the flowing air at sunset, it is better to use the porous media. At 20:00, the air temperature without porous media is greater than that with the porous media. The porous media increase the heat transferred from the absorber to the air and therefore exhausts more quickly the heat stored in the absorber.
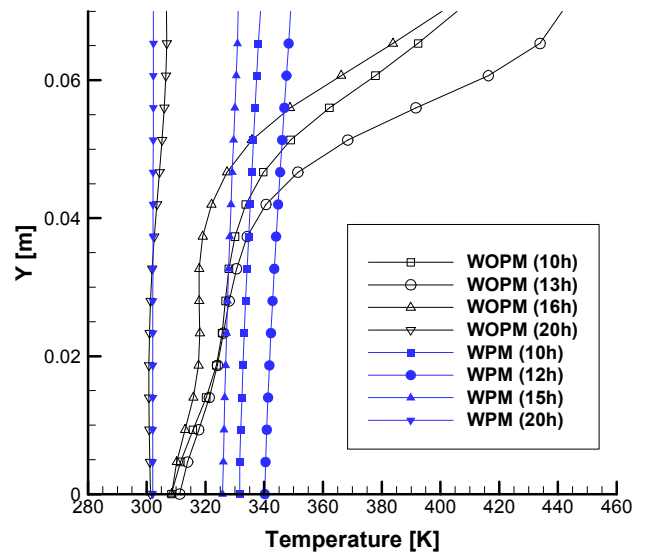
FIG. 17. THE OUTLET TEMPERATURE DISTRIBUTIONS OF AIR IN *y* DIRECTION AT THE SECOND CHANNEL AS A RESULT OF DAILY SOLAR INTENSITY VARIATION.

CONCLUSION

This paper presents numerical analysis of double pass solar air collector with porous material. A comparison with a double pass solar air collector without porous media was developed to see the thermal contribution of the porous media. It is noted that the extended area of the absorber by adding the porous media increases the heat transfer and reduces the absorber temperature. Therefore, the heat energy absorbed from the solar irradiation is distributed throughout the porous media and the absorber plate and dissipated more effectively to the flowing fluid. The foregoing results can be summarized as follows:

1. Without porous media the air temperature in the vicinity of the absorber plate is significantly more higher than that in the bottom and the temperature gradient is enough large. By using the porous media, the average outlet temperature is better and the temperature is almost constant.
2. The temperature of the flowing air through the collector decreased with increased mass flow rate. The higher flow rate reduces the air temperature at the outlet of the air. Thus, the temperature difference between the inlet and the outlet of air decreases with increased flow rate.
3. Without porous media, the increasing of the outlet air temperature with increasing the spacing absorber-insulating plate is much higher than with porous media. This shows that the porous media increases sufficiently the conduction heat transfer where this spacing is reduced.
4. The porous media improves the thermal efficiency by about 13.5 %. This improvement of the thermal efficiency decreases with the increase of the mass flow and reaches about 5.5 %.
5. Comparison between the values of the outlet air temperature with and without the porous media indicated that the maximum values of the outlet air temperature with porous media are less than that without porous media during sunshine hours but have a tendency to maintain the outlet air temperature for a longer time. At 20:00, the air temperature without porous media is greater than that with the porous media. The porous media increase the heat transferred from the absorber to the air and therefore exhausts more quickly the heat stored in the absorber.

NOMENCLATURE

A area of solar air heater (m^2)

c specific heat (J/(kg K))

F inertia coefficient

d_p particle diameters (m)

G rate of solar flux incident on the glass cover (W/m^2)

h convective heat transfer coefficient (W/(m^2K))

H_1 first channel depth (m)

H_2 second channel depth (m)

k permeability of porous media (m^2)

L length of solar air collector (m)

n normal of wall

p pressure (Pa)

q_m mass flow (kg/s)

t time (s)

T temperature (K or °C)

$\overline{T_a}$ average outdoor ambient temperature (°C)

T_r amplitude of the ambient temperature (°C)

u velocity component in x-direction (m/s)

u_{in} velocity inlet (m/s)

v velocity component in y-direction (m/s)

w velocity component in z-direction (m/s)

W width of solar air collector (m)

WPM   with porous media

WOPM   without porous media

V average wind velocity (m/s)

x, y, z cartesian coordinates (m)

Greek symbols

λ thermal conductivity (W/(m K))

μ dynamic viscosity (kg/(m s))

ρ density (kg/m^3)

ε porosity of porous absorber

ε_{ext} emissivity of exterior surface

ε_g emissivity of glass cover

δ thickness (m)

Subscripts

a ambient

ab absorber

eff effective

f fluid

g glass cover

i inlet

o outlet

s solid

sky sky

w wall

REFERENCES

[1] K. Sopian, Supranto, W.R.W. Daud, M.Y. Othman, B. Yatim, Thermal performance of the double-pass solar collector with and without porous media, Renewable Energy 18 (1999) 557-564

[2] K. Sopian, M.A. Alghoul, Ebrahim M. Alfegi, M.Y. Sulaiman, E.A. Mus, Evaluation of thermal efficiency of double-pass solar collector with porous–nonporous media, Renewable Energy 34 (2009) 640–645

[3] P. Naphon, Effect of porous media on the performance of the double-pass flat plate solar air heater, International Communications in Heat and Mass Transfer 32 (2005) 140–150.

[4] C.D. Ho, T.C. Chen, The recycle effect on the collector efficiency improvement of double-pass sheet-and-tube solar water heaters with external recycle, Renewable Energy 31 (2006) 953–970

[5] C.D. Ho, T.C. Chen, Collector efficiency improvement of recyclic double-pass sheet-and-tube solar water heaters with internal fins attached, Renewable Energy 33 (2008) 655–664

[6] A.A. El-Sebaii, S. Aboul-Enein, M.R.I. Ramadan, E. El-Bialy, Year round performance of double pass solar air heater with packed bed, Energy Conversion and Management 48 (2007) 990–1003.

[7] M.R.I. Ramadan, A.A. El-Sebaii_, S. Aboul-Enein, E. El-Bialy, Thermal performance of a packed bed double-pass solar air heater, Energy 32 (2007) 1524–1535

[8] B.M. Ramani, Akhilesh Gupta, Ravi Kumar, Performance of a double pass solar air collector, Solar Energy 84 (2010) 1929–1937

[9] C.D. Ho, H.M. Yeh, T.C. Chen, Collector efficiency of upward-type double-pass solar air heaters with fins attached, International Communications in Heat and Mass Transfer 38 (2011) 49–56.

[10] R. Kumar, M.A. Rosen, Performance evaluation of a double pass PV/T solar air heater with and without fins, Applied Thermal Engineering 31 (2011) 1402-1410

[11] S. Chamoli, R. Chauhan, N.S. Thakur, J.S. Saini, A review of the performance of double pass solar air heater, Renewable and Sustainable Energy Reviews 16 (2012) 481–492

[12] J. Hu, X. Sun, J. Xu, Z. Li, Numerical analysis of mechanical ventilation solar air collector with internal baffles, Energy and Buildings 62 (2013) 230–238.

[13] A.L. Hernández, J.E. Quiñonez, Analytical models of thermal performance of solar air heaters of double-parallel flow and double-pass counter flow, Renewable Energy 55 (2013) 380-391

[14] E.A. Musa, K. Sopian and S. Abdullah, "Transient Analysis for a Double-Pass Solar Collector With and Without Porous Media", ASME Solar 2002: International Solar Energy Conference Solar Energy Reno, Nevada, USA, June 15–20, 2002

[15] D. Peng, Z. Chen, Numerical simulation of phase change heat transfer of a solar flat-plate collector with energy storage, BUILD SIMUL 2 (2009) 273–280

[16] C. Xu, Z. Song, L.D. Chen, Y. Zhen, Numerical investigation on porous media heat transfer in a solar tower receiver, Renewable Energy 36 (2011) 1138-1144

[17] F. Wang, Y. Shuai, H. Tan, C. Yu, Thermal performance analysis of porous media receiver with concentrated solar irradiation, International Journal of Heat and Mass Transfer 62 (2013) 247–254.

[18] W. Chen, W. Liu, Numerical analysis of heat transfer in a passive solar composite wall with porous absorber, Applied Thermal Engineering 28 (2008) 1251–1258

[19] J.A. Duffie, W.A. Beckman, Solar Energy Thermal Process, John Wiley and Sons Inc., 1974